Atmos. Meas. Tech. Discuss., doi:10.5194/amt-2016-414, 2017
Manuscript under review for journal Atmos. Meas. Tech.
Discussion started: 14 February 2017

Atmospheric Measurement Techniques Discussions

Precipitable Water Characteristics during the 2013 Colorado Flood using Ground-Based GPS Measurements

Hannah K. Huelsing[1,2], Junhong Wang[2], Carl Mears[3], and John J. Braun[1]

1. Constellation Observing System for Meteorology, Ionosphere, and Climate Program Office
   University Corporation for Atmospheric Research
   3300 Mitchell Lane, Boulder, CO 80301
2. Department of Atmospheric and Environmental Sciences
   University at Albany, SUNY
   1400 Washington Avenue, Albany, NY 12222
3. Remote Sensing Systems
   444 10th Street, #200
   Santa Rosa, CA 95401

Corresponding Author:
Hannah K. Huelsing
Constellation Observing System for Meteorology, Ionosphere, and Climate Program
University Corporation for Atmospheric Research
3300 Mitchell Lane, Boulder, CO 80301
Phone: (303) 497-2606; Email: huelsing@ucar.edu

Atmos. Meas. Tech. Discuss., doi:10.5194/amt-2016-414, 2017
Manuscript under review for journal Atmos. Meas. Tech.
Discussion started: 14 February 2017

Atmospheric Measurement Techniques Discussions

Abstract

During 9th-16th September 2013, the Front Range region of Colorado experienced heavy rainfall that resulted in severe flooding. Precipitation totals for the event exceeded 450 mm, damages to public and private properties were estimated to be over $2 billion, and nine lives were lost. This study analyzes the characteristics of precipitable water (PW) surrounding the event using 10 years of high-resolution GPS PW data in Boulder, Colorado, which was located within the region of maximum rainfall. PW in Boulder is dominated by seasonal variability with an average summertime maximum of 36 mm. In 2013, the seasonal PW maximum extended into early September and the September monthly mean PW exceeded the 99th percentile of climatology with a value 25% higher than the 40 year climatology. Prior to the flood, around 18 UTC on 8 September, PW rapidly increased from 22mm to 32mm and remained around 30mm for the entire event as a result of the nearly saturated atmosphere. The frequency distribution of September PW for Boulder is typically normal, but in 2013 the distribution was bimodal due to a combination of above average PW values from September 1st-15th and much drier conditions from 16th-30th September. The above normal, near saturation PW values during the flood were the result of large-scale moisture transport into Colorado from the eastern tropical Pacific and the Gulf of Mexico. This moisture transport was the product of a stagnating, cutoff low over the southwestern United States working in conjunction with an anticyclone located over the southeastern United States. A blocking ridge located over the Canadian Rocky Mountains kept both of the synoptic features in place over the course of several days, which helped to provide continuous moisture to the storm, thus enhancing the accumulated precipitation totals.

Atmos. Meas. Tech. Discuss., doi:10.5194/amt-2016-414, 2017
Manuscript under review for journal Atmos. Meas. Tech.
Discussion started: 14 February 2017

Atmospheric Measurement Techniques Discussions

Keywords

Precipitable Water, GPS, 2013 Colorado Flood, Extreme Precipitation

Atmos. Meas. Tech. Discuss., doi:10.5194/amt-2016-414, 2017
Manuscript under review for journal Atmos. Meas. Tech.
Discussion started: 14 February 2017

Atmospheric Measurement Techniques Discussions

1. Introduction

During 9th-16th September 2013, multiple local and state precipitation records were broken when low-level, easterly flow interacted with an anomalous moisture pool over the Front Range region of Colorado to produce one of the largest floods in state history (Colorado Climate Center, 2013). The heaviest and most persistent rainfall occurred on the 11th and 12th of September, with a maximum centered over Boulder and Larimer counties (Fig. 1). In the hardest hit areas, total precipitation accumulation exceeded 450 mm (17.7 in) (Gochis et al. 2015). The city of Boulder set multiple records, observing 292.6 mm over the course of two days and 341.8 mm over the course of three days. The resultant flooding claimed nine lives and caused 1,100 documented landslides. Damages to public and private properties were estimated to be over $2 billion (Gochis et al. 2015).

The following summary of the September 2013 event was first presented in Gochis et al. (2015). Surface temperatures were in the 16-18 °C (60-64 °F) range and precipitable water (PW) values were high. Periods of heavy precipitation exceeding 25 mm (1 in) per hour, along with flooding, began on the evening of 11th September, with the heaviest portions over the Front Range, the area outlined in Fig. 1. The mountainous region between Boulder and Estes Park experienced the heaviest rain rates, which ranged from 25-50 mm (1-2 in) per hour and resulted in an overnight total exceeding 200 mm (8 in). Somewhat lighter rainfall continued into the 12th, becoming intense once more during the afternoon hours and increasing rainfall totals to over 380 mm (15 in) in the Boulder to Estes Park region. By the 13th, precipitation had finally lessened to intermittent showers and widespread drizzle, finally clearing on the 14th. A final surge of

Atmos. Meas. Tech. Discuss., doi:10.5194/amt-2016-414, 2017
Manuscript under review for journal Atmos. Meas. Tech.
Discussion started: 14 February 2017

93 moisture occurred on the 15th and resulted in 25-50 mm (1-2 in) of widespread, moderate
94 rainfall on soils that were already saturated, thus increasing the amount of runoff.
95 This event was uncharacteristic, not only because of its rainfall amounts but also
96 because of the time of year in which it occurred. Petersen et al. (1999) examined the
97 climatology of precipitation events over the Front Range region and found that, while a
98 majority of events occur between April and October, the convective classification of the
99 events differ depending on what time of year they occur in. There are two peaks in the
100 event distribution, the first of which occurs in late May to early June. Precipitation events
101 during this time are synoptic, or large, scale and quasi-stationary. The precipitation in
102 these events is enhanced orographically and locally, and is typically widespread and of
103 moderate intensity. The second peak in precipitation events occurs from late July into
104 early September with a pronounced maximum frequency from late July into early
105 August. The storms in these events generally have a small areal extent and are highly
106 convective. The September 2013 event was quasi-stationary and synoptic with
107 precipitation controlled by localized and orographic enhancements. The areal extent of
108 the 2013 event was large and the rainfall was of moderate intensity. According to the
109 climatology completed by Petersen et al. (1999), this type of event was more typical of
110 storms which occur in late May to early June. However, this event occurred at a time of
111 year when precipitation tends to be highly convective and of small areal extent, so the
112 timing, as well as the amount of rainfall, was abnormal.
113 In another study which examined the climatology of rainfall events in Colorado,
114 Mahoney et al. (2015) found that the region of Colorado east of the Continental Divide
115 does not generally experience heavy precipitation events in the fall because it is during

Atmos. Meas. Tech. Discuss., doi:10.5194/amt-2016-414, 2017
Manuscript under review for journal Atmos. Meas. Tech.
Discussion started: 14 February 2017

Atmospheric Measurement Techniques Discussions

this time of year that the region experiences seasonal atmospheric drying. They did note that there was enhanced climatological variability in September and October, making it difficult to place these months into the same category as the drier months (November-February). In general, east of the Continental Divide experiences most of its precipitation in the spring and summer months, with the Front Range receiving a majority of its moisture in the spring. However, extreme precipitation events are not limited to these seasons and can also occur in fall and winter months.

Flooding due to extreme precipitation events can occur at any time of the year because all elevations in all seasons are prone to experiencing heavy precipitation. This is partially represented by the dates in Table 1, which compares the September 2013 event to previous heavy precipitation events in Northern Colorado history that resulted in catastrophic flooding (Colorado Climate Center; Maddox et al. 1977; Petersen et al. 1999; Gochis et al. 2015). Prior to the September 2013 event, there were 5 events on record that were classified as comparable to the 2013 event by the Colorado Climate Center. However, all except one of these storms took place in the spring and summer months, as would be expected from the climatology of the rainfall events presented in earlier.

Out of the events listed in Table 1, the Colorado Climate Center noted that the event that occurred on 1st-12th September 1938 near Fort Collins, Colorado was the most similar in timing and magnitude to the September 2013 event. Observers recorded 8-10 inches of rainfall and the surrounding region experienced severe flooding. However, there is not much else known about this event because the amount of recorded atmospheric data available from this time period is limited. Comparing the September

Atmos. Meas. Tech. Discuss., doi:10.5194/amt-2016-414, 2017
Manuscript under review for journal Atmos. Meas. Tech.
Discussion started: 14 February 2017

Atmospheric Measurement Techniques Discussions

2013 event to the 5 previous events in Table 1, this event had the highest total rainfall and caused the most damage, as is seen by the total cost of the event. This event also had a vast areal coverage, with heavy precipitation occurring from Denver all the way into southern Wyoming. Flooding took place as far to the east as Nebraska and caused a lot of damage to infrastructure along the Front Range of Colorado.

The amount of precipitation that fell during the September 2013 event required a large amount of moisture at a time when atmospheric moisture was beginning to decrease from higher summer values (Mahoney et al., 2015). Moisture transport and quantity are important aspects to evaluate when investigating heavy precipitation events. However, there has not been a vast amount of research examining the characteristics of PW during heavy precipitation events. Such characteristics are important to understand because they could influence future weather and climate trends. Kunkel et al. (2013) found an increasing trend in atmospheric PW quantities associated with extreme precipitation events and suggested this trend could lead to an increase in storm intensity. While Hoerling et al. (2014) noted that the September 2013 event was probably not connected to climate change, they did find that heavy precipitation events are becoming more frequent and Karl and Trenberth (2003) found evidence that the number of heavy precipitation events is expected to increase with increasing global temperatures, such as we are experiencing now. The observed and projected increase in the number of heavy precipitation events, combined with the uncertainty of how PW contributes to characteristics of these events, motivated an investigation of PW characteristics surrounding the 2013 event so as to better understand the contributions of PW to an

Atmos. Meas. Tech. Discuss., doi:10.5194/amt-2016-414, 2017
Manuscript under review for journal Atmos. Meas. Tech.
Discussion started: 14 February 2017

161 extreme precipitation event with the objective to someday apply these results to future
162 research incorporating a wider variety of events.
163 As the aim of this research was to examine the characteristics of atmospheric PW
164 during the 2013 Colorado Flood, data with a high spatial and temporal resolution was
165 needed to resolve features within the event. GPS receivers are much more densely spaced
166 with a total of 236 stations over North America than the radiosonde network, which has a
167 total of 92 stations. The higher density of observations in the GPS network results in a
168 higher spatial resolution with which to analyze storm features and water vapor transport.
169 GPS data also has a much higher temporal resolution of anywhere from 30 minutes to
170 two hours, as compared to the standard, twice-daily launching of radiosondes.
171 The primary goal of this research was to investigate the magnitude and characteristics
172 of PW over the Front Range region associated with the September 2013 event. The goal
173 of this study was to answer the following scientific questions.
174 (1) What were the characteristics of PW surrounding this event? This portion of
175 research was focused on the examination of the temporal variability of PW, as
176 well as a comparison with climatology, before, during, and after the event.
177 (2) Where did the moisture for the 2013 event originate? To answer this question,
178 synoptic-scale dynamics and pre-existing conditions that led to large-scale,
179 continuous moisture transport were evaluated.

180 **2. Data and Methodology**

181 *2.1 Precipitable Water Datasets*

182 Two datasets were used to analyze PW characteristics surrounding the 2013 event.
183 The first of these was a two-hourly, long-term (1995-2015) PW dataset (Wang et al.

Atmos. Meas. Tech. Discuss., doi:10.5194/amt-2016-414, 2017
Manuscript under review for journal Atmos. Meas. Tech.
Discussion started: 14 February 2017

2007; Mears et al. 2015; Mears et al. 2016). The PW in this dataset is derived using 5-minute International Global Navigation Satellite System (GNSS) Service (IGS) Zenith Total Delay (ZTD) data. The analysis technique for the interpolation and conversion of ZTD to PW is summarized in Wang et al. (2007) and two key variables used in the conversion are water-vapor-weighted atmospheric temperature (Tm) and surface pressure (Ps). ZTD is represented as the sum of the Zenith Hydrostatic Delay (ZHD), which is a function of Ps, and the Zenith Wet Delay (ZWD), which is a function of PW and Tm. The 2-hourly PW data from Boulder became available starting in 2004.

The second PW dataset used in this study was the 30-minute SuomiNet dataset from the Constellation Observing System for Meteorology, Ionosphere, and Climate (COSMIC) group (Ware et al. 2000). The SuomiNet network currently consists of over 200 sites located around North America and the data are processed in near-real time from raw GPS data, the values of which do not differ greatly from post-processed GPS data. For this research, the standardized anomalies of the SuomiNet data were calculated by subtracting PW at each time step from the mean and dividing this by the standard deviation (Grumm and Hart 2001). The standardized anomaly data were gridded and interpolated using a general kriging method to a grid box of 0.5°X0.5°. Kriging is defined as optimized interpolation that is weighted by spatial covariance values and based on regression against observed values of surrounding data points (Bohling 2005). This method was chosen because of its simplicity and superior performance when compared with the inverse distance weighting (IDW) method (Zimmerman et al. 1999; Yasrebi et al. 2009).

Atmos. Meas. Tech. Discuss., doi:10.5194/amt-2016-414, 2017
Manuscript under review for journal Atmos. Meas. Tech.
Discussion started: 14 February 2017

2.2 Formulation of a GPS PW Climatological Dataset

PW data for Boulder, Colorado were chosen to evaluate the PW variability of this region over the course of 10 years and compare this variability with that of 2013 to improve the understanding of how the September 2013 event differed from climatology. This region encompasses six SuomiNet stations and two IGS stations (Fig. 1a). To examine the anomalous nature of the flood, a dataset with a length of at least 10 years of observations was needed as a climatological standard for the analyzed region. While 10 years is not long enough for a standard climatology of 30 years as defined by the World Meteorological Organization (WMO), GPS PW data for Boulder has only been available since 2004. The PW time series of each GPS station was initially examined to determine which, if any, station had a long enough data record to serve as the climatological standard, and also to check for data outliers and data continuity. No stations were found to have more than seven years of data and datasets that contained discontinuities were discarded. A major issue that appeared during this analysis was that only one SuomiNet and one IGS station had data observations during the September 2013 event, and neither of them had a lengthy dataset. A decision was made to combine the data from different stations in the region and make a 10-year dataset that included observations from the flood.

The GPS PW data used to create the 10-year dataset were first quality-controlled by using several methods defined in Wang et al. (2007). The first method used was the range test in which the lower and upper limits of PW values were set as 0mm and 150mm, respectively. The second quality-control method used involved using the mean and standard deviation for each month to detect any outliers. This method required that at

least one-quarter of the data be present in order to have an adequate amount of observations so that the statistical aspects could be deemed accurate. Individual PW values within each month were analyzed and any values that were more than 4 standard deviations away from the monthly mean were discarded (Wang et al. 2007). The quality control removed 0.1% of the total data points for the station SA00 and less than 0.1% of the total data points for the rest of the stations.

The next step in the creation of the 10-year dataset was to compare PW data among the stations. PW is strongly dependent on elevation so any station that had an elevation above 1,800 m was eliminated because these receivers were located too far above the elevation of Boulder (1655 m). To remain consistent, the remaining stations were compared to the station with the longest dataset and elevation closest to that of Boulder (DSRC). Five stations were chosen for the merged 10-year PW dataset (Fig. 2) because their averaged PW differences were not statistically significant from one another and the elevation differences between all stations were less than 50 m. A more thorough analysis of the complete dataset and its comparison with 2013 is described in Sect. 3. The SuomiNet station, P041, also passed the statistical significance test, but did not have a complete record of data for 2013 so could not be included in the 10-year dataset. Instead, the 2013 PW data from P041 was used to analyze small-scale variability leading up to, and during, the flood period because it has a higher temporal resolution (30 minutes) than NIST (two-hourly), which was chosen for the 10-year dataset.

2.3 Additional Datasets

The data used as a long-term PW climatology dataset were twice-daily radiosonde data from the Stapleton airport in Denver, Colorado extracted from the homogenized

Atmos. Meas. Tech. Discuss., doi:10.5194/amt-2016-414, 2017
Manuscript under review for journal Atmos. Meas. Tech.
Discussion started: 14 February 2017

Atmospheric Measurement Techniques Discussions

radiosonde dataset created by Dai et al. (2011) (Fig. 1b). This PW dataset was created by integrating specific humidity from the surface to 100hPa, is available from 1979 to 2013, and was homogenized using an advanced statistical approach that is more thoroughly described in Dai et al. (2011).

The primary dataset used to evaluate moisture transport was the North American Regional Reanalysis (NARR) dataset, which is available from 1979 to the present (Mesinger et al. 2006). The domain for NARR is North America and the horizontal resolution is 32 km with 45 vertical layers. The NARR variables chosen for the evaluation of moisture transport surrounding the event were the 500 hPa geopotential height and the vertically integrated moisture flux.

3. Precipitable Water Characteristics

Gochis et al. (2015) noted that the atmosphere over Northern Colorado was abnormally moist from 9th-16th September. Radiosondes captured PW values above 30 mm, an abnormal value for a semi-arid climate. Gochis et al. (2015) also noted that the raindrop distribution during the event consisted of numerous small raindrops, which is more commonly observed in a tropical climate. To better understand how abnormal the atmospheric moisture was during this event, the magnitude, distributions, and variability of PW over Boulder were evaluated and compared to climatology.

3.1 Temporal Variability of Precipitable Water

First, the temporal characteristics of September of 2013 were compared with the 10-year GPS PW dataset described in Sect. 2.2. Figure 2 shows the time series of the merged 10-year PW dataset discussed in Sect. 2. The strongest PW variation is seasonal with a mean seasonality of 18mm and the summer peaks are coincident with the annual

Atmos. Meas. Tech. Discuss., doi:10.5194/amt-2016-414, 2017
Manuscript under review for journal Atmos. Meas. Tech.
Discussion started: 14 February 2017

occurrence of the wet season in Colorado. Also note that the belted appearance of this time series represents synoptic and diurnal PW variability, the latter of which has an average magnitude of 8 mm. The maximum value of PW for 2013 was 33.5 mm on September 12. Note the extension of high PW values from the summer months into early September of 2013. This extension is not observed in any of the other years contained in this dataset and is an indication that the atmosphere was anomalously moist for the time of year in which the flood occurred.

Figure 3 zooms in on the extension of high PW values observed in September of 2013, giving a clearer view of the temporal variability of PW surrounding the flood event. The high PW values from 28th August - 5th September represent moisture associated with the end of the North American Monsoon. These high values begin to decrease around 6th September before quickly rising on September 9th into the 10th, with values spiking to above 30 mm. PW decreases slightly to 26 mm until the 11th, when it once again increases to above 30 mm where it remains until the 13th. After this, PW decreases to values closer to the September climatological average of 15 mm. An interesting point to take note of is that PW values stay relatively constant during the event despite the fact that continuous, and sometimes heavy, precipitation is occurring. For PW to remain at high values over multiple days, as was seen here, moisture needed to be continuously transported into the region (Gimeno et al. 2012). Had there not been a constant transport of moisture, PW would have decreased as atmospheric moisture condensed and formed precipitation. The examination of the moisture transport that fueled this event is presented in Sect. 4.

Atmos. Meas. Tech. Discuss., doi:10.5194/amt-2016-414, 2017
Manuscript under review for journal Atmos. Meas. Tech.
Discussion started: 14 February 2017

299 *3.2 Precipitable Water Abnormality During the 2013 Flood*

300 The consistently high values of PW during the time of heaviest precipitation in
301 Fig. 3 led to an investigation to discern if the atmosphere over Boulder was fully
302 saturated during the September 2013 event. To evaluate this, observed radiosonde PW
303 data were compared with PW values that were calculated assuming a fully saturated
304 atmosphere, i.e. 100% relative humidity from the surface up to 300 hPa. Figure 4 shows
305 the comparison between these two variables from 6th-20th September 2013. Starting on
306 10th September observed and fully saturated PW values were within 5 mm of each other,
307 indicating an atmosphere that was very near to saturation during the course of the
308 September 2013 event. Except for a period of time on 14th September when the
309 atmosphere began to dry, observed PW stayed relatively close in value to the fully
310 saturated PW until 16th September.

311 Figure 5 compares monthly-averaged 2013 GPS data and radiosonde data to 40 and 10
312 years of monthly-averaged radiosonde and GPS data, respectively. 2013 PW monthly
313 averages were consistently lower than climatology until July. Up until July, the Front
314 Range was still under drought conditions according to the National Climatic Data Center
315 (NCDC) North American Drought Monitor. The monthly average for September of 2013
316 was around 20 mm, approximately 25% higher than the long-term climatological monthly
317 average for September. Also note that the monthly average for September of 2013 is
318 above the 95th and 99th percentiles, which were calculated from 40 years of monthly-
319 averaged radiosonde data. McKee and Doesken (1997) evaluated extreme precipitation
320 events for Colorado from the late 1800's up until 1996 and found that, for these events,
321 PW never exceeded the 95th percentile. That the monthly averaged PW for September of

Atmos. Meas. Tech. Discuss., doi:10.5194/amt-2016-414, 2017
Manuscript under review for journal Atmos. Meas. Tech.
Discussion started: 14 February 2017

Atmospheric Measurement Techniques Discussions

2013 exceeded the 99th percentile when compared to 40 years of data shows just how anomalous the event was in terms of PW magnitude and timing.

Another tool used to evaluate how anomalous the 2013 Event was in terms of PW was to examine the PW frequency distributions. Foster et al. (2006) examined the monthly and annual frequency distributions of PW data for various stations and found that there were three main types of distributions for PW data: lognormal, which is the most common distribution around the world; reverse-lognormal, which represents an atmosphere near saturation; and bimodal, which occurs in regions with strong seasonal variability such as monsoonal zones.

To analyze PW frequency for this event, monthly distributions were created for June through September of 2004-2013 (Fig. 6). The skewness of each distribution was then calculated and these values, along with visual analysis, were used to determine if each distribution was normal, lognormal, reverse-lognormal, or bimodal. Bulmer (1979) provided guidelines for interpreting the skewness of a distribution that were employed when evaluating the distributions in this study. A normal distribution has a skewness from -0.5 to 0.5, while a positive (negative) skewness with its absolute values within 0.5 to 1 represents a lognormal (reverse-lognormal) distribution (Bulmer 1979; Foster et al. 2006).

Upon analyzing the distributions in Fig. 6, June through September primarily have normal distributions with September being, on average, slightly more positively skewed than the other months with a value of 0.32, although the distribution is still considered normal according to the conditions for skewness defined in Bulmer (1979). However, the seasonal variation in PW is still evident as July and August distributions

Atmos. Meas. Tech. Discuss., doi:10.5194/amt-2016-414, 2017
Manuscript under review for journal Atmos. Meas. Tech.
Discussion started: 14 February 2017

345 tend to have their highest frequencies over higher values of PW than either June or
346 September. Also, despite most months having a normal distribution, there are four
347 distributions which were labeled as lognormal because they have skewness values larger
348 than 0.5: July 2005, September 2008, September 2010, and June 2013.

349 The distribution that shows the largest shift in distribution from the other years is that
350 of September of 2013, which had a bimodal distribution. Figure 7 shows a more detailed
351 comparison of September of 2013 PW data with 10 years of GPS PW data and 40 years
352 of radiosonde PW data. September of 2013 PW data were split up into two categories:
353 "Flood", which represents 1st-15th September; and "Post-Flood", which represents 16th-
354 30th September. Fig. 7 shows how different September of 2013 is from climatology and
355 also how the atmosphere during the "Flood" differed from the "Post-Flood" atmosphere.
356 The atmosphere during the "Flood" was highly saturated, with a peak frequency around
357 25 mm and PW values as high as 35 mm. The frequency distribution during this time was
358 normal with a skewness value of 0.175. The "Post-Flood" atmosphere had a distinct
359 lognormal distribution indicated by visual analysis and also by a skewness of 0.6838. The
360 atmosphere at this time was considerably drier, with frequency peaking at 0.9 around
361 7 mm of PW.

362 **4. Water Vapor Transport**

363 The occurrence of heavy precipitation such as was observed during the September
364 2013 event requires sufficient moisture supply to fuel it. In Sect. 3, PW was shown to
365 spike rapidly prior to the flood and remain at highly anomalous values for the duration of
366 the event. In order to more completely understand the PW characteristics of this event, it
367 was important to investigate where the moisture originated and what mechanisms were

Atmos. Meas. Tech. Discuss., doi:10.5194/amt-2016-414, 2017
Manuscript under review for journal Atmos. Meas. Tech.
Discussion started: 14 February 2017

Atmospheric Measurement Techniques Discussions

368 controlling the moisture transport that kept the atmosphere very near to saturation for
369 seven consecutive days.

370 The moisture source and transport for the September 2013 event was briefly
371 investigated in previous literature. Gochis et al. (2015) noted that the sources of moisture
372 for the event were the Gulf of Mexico and the eastern tropical Pacific Ocean, both of
373 which had 1-3 °C above normal sea surface temperature (SST) anomalies. They stated
374 that the moisture from these regions was transported into the Front Range by a cutoff low
375 over the southwestern United States working in conjunction with an anticyclone over the
376 southeastern United States. Both of these features were kept in place for multiple days by
377 a blocking ridge located over the Canadian Rockies (Gochis et al. 2015). Trenberth et al.
378 (2015) stated that the source of moisture for the September 2013 event was only from the
379 eastern tropical Pacific Ocean, while Mahoney et al. (2015) claimed the moisture for the
380 event came primarily from the Gulf of Mexico.

381 Due to the slight variation of opinion on which body of water was the source of
382 moisture for the event, this study further investigates moisture source and transport by
383 examining NARR 500 hPa geopotential height and integrated water vapor flux in
384 conjunction with the standardized anomaly of gridded SuomiNet PW data. Five times
385 surrounding the event were chosen for analysis based on their proximity to rapid
386 fluctuations in PW (Fig. 3). The three variables listed above are plotted in Fig. 8 at each
387 of the five time steps.

388 Figure 8a-c shows the atmospheric conditions on 6th September at 9 UTC, prior to
389 the start of the event. There was a large ridge with 500 hPa geopotential heights above
390 596 gpm over the western half of the United States (US) (Fig. 8a) which contributed to

Atmos. Meas. Tech. Discuss., doi:10.5194/amt-2016-414, 2017
Manuscript under review for journal Atmos. Meas. Tech.
Discussion started: 14 February 2017

Atmospheric Measurement Techniques Discussions

391 higher temperatures and dried the atmosphere over Boulder as seen in Fig. 8c. At that
392 point, there was no direct water vapor transport from either the Gulf of Mexico or the
393 eastern Pacific (Fig. 8b).
394 Moving on to 9th September at 18 UTC (Fig. 8d-f), a trough started to form over
395 the western United States and an anticyclone shifted over the southeastern US (Fig. 8d).
396 Together, these began transporting water vapor towards the northeast along the eastern
397 flank of the trough from the eastern Pacific (Fig. 8e). This transport contributed to a belt
398 of PW anomalies with magnitudes of 1.5 to 2.5 standard deviations over the southwestern
399 and western US (Fig. 8f). The PW anomaly over Boulder at that point was between 1-1.5
400 standard deviations and precipitation had not yet begun (Fig. 9). Water vapor appeared to
401 travel to Colorado from the eastern Tropical Pacific at that time (Fig 8e).
402 By 11th September at 6 UTC (Fig. 8g-i), the low pressure over the western US
403 deepened and formed into a cut-off low (Fig. 8g). The low stagnated over the western US
404 due to the influence of the blocking ridge under which it resided. The anticyclone over
405 the eastern US also strengthened. Working in conjunction, the strengthening of the low
406 and the high increased the southerly water vapor transport and there was a corridor of
407 flux convergence over New Mexico and the direction of the flux over Northern Colorado
408 was toward the Rocky Mountains (Fig. 8h). This resulted in a corridor of PW anomalies
409 that stretched from the Mexican border to southern Wyoming (Fig. 8i). The magnitude of
410 the PW anomaly over Boulder rose to between 2.5 to 3 standard deviations as the
411 moisture pooled against the Rocky Mountains due to easterly water vapor transport.
412 Light, orographically enhanced precipitation began and Boulder experienced rain rates

around 5mm h^{-1} (Fig. 9). Water vapor was being transported into Colorado from the eastern Tropical Pacific and the Gulf of Mexico at this time (Fig 8h).

By 12th September at 6 UTC (Fig. 8j-l), the anticyclone began to break down but the cutoff low deepened even further (Fig. 8j). Water vapor was still being transported into the region from the Gulf of Mexico by the synoptic conditions with an easterly component of the flux continuing to pool water vapor against the Rocky Mountains (Fig. 8k). However, the transport of moisture into Colorado appeared to have weakened substantially and the eastern Tropical Pacific was no longer a source of moisture. There was still a corridor of PW anomalies coinciding with the regions of strong water vapor flux and the magnitude of the anomaly over Boulder was still between 2.5 to 3 standard deviations (Fig. 8l). Precipitation intensified over the past 24 hours and Boulder experienced up to 35mm h^{-1} of rainfall (Fig. 9). While a majority of the rainfall was orographically-enhanced, the occasional intense periods of rainfall were a result of mesoscale circulations, as was noted by Gochis et al. (2015).

By 14th September at 21 UTC (Fig. 8m-o), the blocking ridge broke down, which allowed synoptic conditions to shift eastward, and the cutoff low once again became a trough (Fig. 8m). This resulted in the water vapor flux also shifting eastward (Fig. 8n). The PW anomaly over Boulder decreased to between 1 to 2 standard deviations (Fig. 8o). Rainfall for the event ended at this point, excluding a peak that occurred during the afternoon of 15th September (Fig. 9).

Upon comparing NARR integrated moisture flux with 500 hPa geopotential height and observed standardized PW anomalies, it was found that the strength and location of moisture transport varied over the course of the event. Prior to the event, on

436 9th September, moisture from the eastern tropical Pacific appears to have been transported
437 up to Colorado by a stagnating cutoff low over the southwestern US. Starting on 10th
438 September, the cutoff low and subtropical anticyclone promoted southerly flow into
439 Colorado from the eastern tropical Pacific and the Gulf of Mexico. As of the 12th
440 September, the eastern tropical Pacific no longer provided moisture for the event and the
441 Gulf of Mexico was the sole source of moisture. By the 14th September, the transport of
442 moisture into Colorado had significantly weakened due to the eastward shift of the
443 synoptic pattern. The moisture transport was dependent on the strength and location of
444 the dominant synoptic features, and based on the analysis shown in Fig. 8 the moisture
445 has been transported into Colorado from both the Eastern Tropical Pacific and the Gulf of
446 Mexico. These results are most consistent with the findings of Gochis et al. (2015), but
447 do not discount the results found in Trenberth et al. (2015) and Mahoney et al. (2015).

448 **5. Conclusions**

449 The aim of this research was to analyze PW characteristics surrounding the
450 September 2013 event and compare them to climatology. Monthly averaged PW values
451 in the GPS dataset for September of 2013 was above the 99th percentile when compared
452 to the climatological data as well as around 25% higher than the monthly-averaged
453 climatological mean value for September. That the monthly average for September of
454 2013 was so far above the climatology for 10 and 40 years of data indicates how
455 anomalous the atmospheric moisture content was during the event. The frequency
456 distribution of PW for September of 2013 was bimodal, which was much different than
457 the typical normal distribution observed in September of other years. Upon further
458 analysis, it was noted that the highly saturated portion of the bimodal distribution was

459 solely the result of the September 2013 event, which had a nearly saturated atmosphere.
460 The second half of September had a lognormal distribution, representing a much drier
461 atmosphere for the rest of the month. The moisture for the event originated from the
462 eastern tropical Pacific at the beginning of the event 9th September, came from this source
463 and the Gulf of Mexico during the heaviest precipitation (10th – 12th September), and then
464 from only the Gulf of Mexico towards the end (12th-14th September).

465 **Code Availability**

466 Code is available from the lead author upon request.

467 **Data Availability**

468 Two-hourly GPS PW data is available upon request from the first and second authors. 30
469 minute SuomiNet GPS PW data is available for download in ASCII and NetCDF format
470 from the COSMIC group website (suominet.ucar.edu). The twice daily, homogenized
471 radiosonde data is available upon request from the second author. NARR data is available
472 for download on the National Oceanic and Atmospheric Administration (NOAA) website
473 (nomads.ncdc.noaa.gov/data/narr). The 1-hourly rain gauge data is available upon request
474 from the National Center for Atmospheric Research (NCAR) Research Applications
475 Laboratory (RAL).

476 **Author Contribution**

477 The first author was the primary researcher with constant assistance and guidance from
478 the second author. The third author was the PI on the grant and a contributing editor. The
479 fourth author served as an editor.

480 **Competing Interests**

481 There are no competing interests from any of the authors.

Disclaimer

There is no disclaimer regarding the research completed in this paper.

Acknowledgements

This research was supported by the National Aeronautics and Space Administration (NASA) RSS Subcontract #6003 under the Prime Contract NNX11AO25A. The first author would like to thank Heather Davis, Rebecca Steeves, Sarah Ditchek, Molly Smith, Rich and Brenda Dixon, Michael Fischer, Joshua Alland, Matthew Vaughan, Casey Peirano , Eric Adamchick, and Ted Letcher for their valuable input and support.

Works Cited

Bohling, G., 2005: Introduction to geostatistics and variogram analysis C&PE 940. Kansas Geol. Surv.

Bulmer, M. G., 1979. Principles of Statistics. Cambridge, MA: M.I.T. Press.

Colorado Climate Center, Colorado Flood 2013 Storm Page, published online October 2013.

Dai, A., J. Wang, P.W. Thorne, D.E. Parker, L. Haimberger, and X.L. Wang, 2011: A new approach to homogenize daily radiosonde humidity data. J. Climate, 24, 965-991.

Foster, J., M. Bevis, and W. Raymond, 2006: Precipitable water and the lognormal distribution. J. Geophys. Res.,111.D15102, doi:10.1029/2005JD006731.

Gimeno, L., A. Stohl, R. M. Trigo, F. Dominguez, K. Yoshimura, L. Yu, A. Drumond, A. M. Durán-Quesada, and R. Nieto (2012), Oceanic and terrestrial sources of continental precipitation, Rev. Geophys., 50, RG4003, doi:10.1029/2012RG000389.

505 Gochis, D., and Coauthors, 2015. The Great Colorado Flood of September 2013. The
506 Bulletin of the American Meteorological Society.
507 Hoerling, M., and Coauthors, 2014: Northeast Colorado extreme rains interpreted in a
508 climate change context [in "Explaining Extremes of 2013 from a Climate
509 Perspective"]. Bull. Amer. Meteor. Soc., 95 (9), S15–S18.
510 Karl, T. R., and K. E. Trenberth, 2003: Modern global climate
511 change. Science, 302, 1719–1723.
512 Kunkel, K. E., and Coauthors, 2013: Monitoring and understanding trends in extreme
513 storms: State of knowledge. Bull. Amer. Meteor. Soc., 94, 499–514.
514 Maddox, R. A., Caracena, F., Hoxit, L. R., Chappell, C. F., 1977: Meteorological Aspects
515 of the Big Thompson Flash Flood of 31 July 1976. NOAA Technical Report.
516 Mahoney, K., Ralph, F. M., Wolter, K., Doesken, N., Dettinger, M., Gottas, D., Coleman,
517 T., White, A., 2015: Climatology of Extreme Daily Precipitation in Colorado and
518 Its Diverse Spatial and Seasonal Variability. Journal of Hydrometeorology.
519 McKee, T. B., and N. J. Doesken, 1997: Final report: Colorado extreme precipitation data
520 study. Climatology Rep. 97-1, Department of Atmospheric Science, Colorado
521 State University, 107 pp. Available from Colorado Climate Center, Department of
522 Atmospheric Science, Colorado State University, Fort Collins, CO 80523.
523 Mears, C, Ho, S., Peng, L., Wang, J., and Huelsing, H., 2015: Total column PW, in State
524 of the Climate in 2014. Bull. Amer. Meteorol. Soc., 96, S22-23.
525 Mears, C, Ho, S., Wang, J., Huelsing, H., and Peng, L., 2016: Total Column PW. Bull.
526 Amer. Meteorol. Soc., In Press.

527 Petersen, W.A., 1999: Mesoscale and Radar Observations of the Fort Collins Flash Flood
528 of 28 July 1997. Bulletin of the American Meteorological Society. Vol. 80, No. 2,
529 February 1999.
530 Wang, J., Zhang, L., Dai, A., Van Hove, T., and Van Baelen, J., 2007: A near-global, 2-
531 hourly dataset of atmospheric precipitable water from ground-based GPS
532 measurements. J. Geophys. Res., 112, D11107, doi:10.1029/2006JD007529
533 Ware, R. H., D. W. Fuller, S. A. Stein, D. N. Anderson, S. K. Avery, R. D. Clark, K. K.
534 Droegemeier, J. P. Kuettner, J. B. Minster, and S. Sorooshian, 2000: SuomiNet: A
535 Real-Time National Network for Atmospheric Research and Education. Bulletin
536 of the American Meteorological Society, 81, 4, 677-694.
537 Yasrebi J, Saffari M, Fathi H, Karimian N, Moazallahi M, et al., 2009. Evaluation and
538 comparison of ordinary kriging and inverse distance weighting methods for
539 prediction of spatial variability of some soil chemical parameters. Research
540 Journal of Biological Sciences 4: 93–102.
541 Zimmerman, D., Pavlik, C., Ruggles, A. and Armstrong, M. P., 1999. An experimental
542 comparison of ordinary and universal Kriging and inverse distance weighting.
543 Mathematical Geology, 31 (4).
544
545
546
547
548
549

Atmos. Meas. Tech. Discuss., doi:10.5194/amt-2016-414, 2017
Manuscript under review for journal Atmos. Meas. Tech.
Discussion started: 14 February 2017

Atmospheric Measurement Techniques Discussions

Date	Location Most Affected	Total Rainfall (inches)	Deaths	Cost
September 1-12, 1938	Fort Collins	8-10	N/A	N/A
May 4-9, 1969	West of Denver	6-9	0	$136.5 million
July 31-August 1, 1976	Estes Park	12-14	144	$348.5 million
July 27-August 4, 1997	Fort Collins	14.5	5	$290 million
April 29-30, 1999	Northern Colorado	8-10	0	$140 million
September 9-16, 2013	Boulder	16	8	$2 billion

Table 1. A comparison of the September 2013 Event to previous flood inducing, heavy precipitation events in Northern Colorado history. All monetary values were calibrated to 2013 values.

Atmos. Meas. Tech. Discuss., doi:10.5194/amt-2016-414, 2017
Manuscript under review for journal Atmos. Meas. Tech.
Discussion started: 14 February 2017

Atmospheric Measurement Techniques Discussions

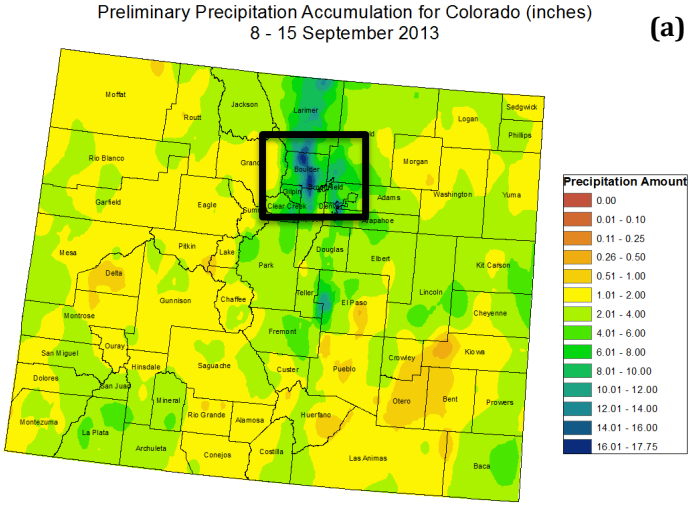

554

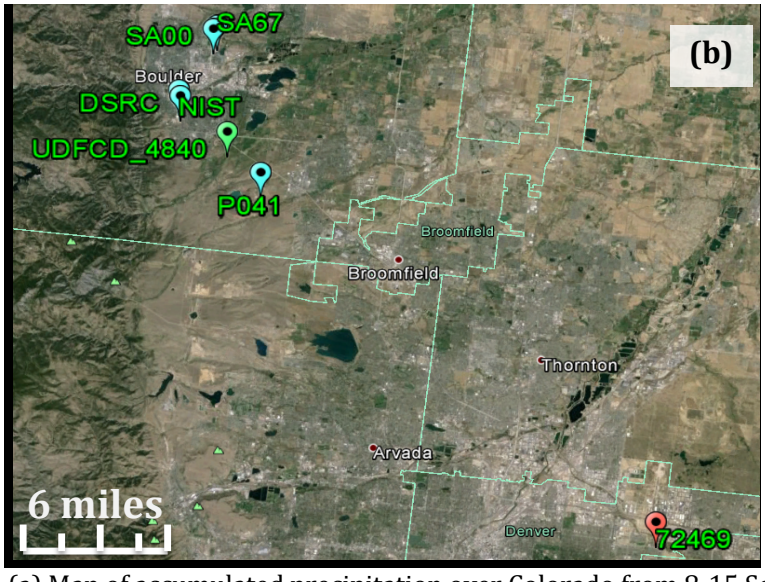

555

556 **Figure 1.** (a) Map of accumulated precipitation over Colorado from 8-15 September
557 2013 (image courtesy of the Colorado Climate Center) with the area depicted in (b)
558 outlined in the black box; and (b) the locations of the primary GPS (blue circles),
559 rain gauge (green circle), and radiosonde (red circle) observations used in this
560 study. NISU and NIST are the only IGS GPS stations plotted on this map. All of the
561 other GPS stations are from the SuomiNet network.

Atmos. Meas. Tech. Discuss., doi:10.5194/amt-2016-414, 2017
Manuscript under review for journal Atmos. Meas. Tech.
Discussion started: 14 February 2017

Atmospheric Measurement Techniques Discussions

562

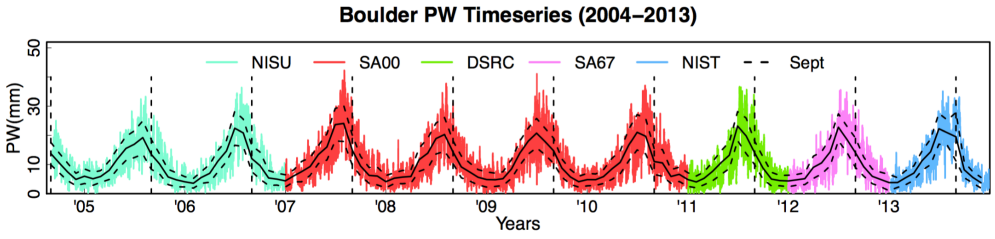

563
564 **Figure 2.** A time series of the GPS PW data for Boulder, Colorado from 2004-2013
565 with each station denoted by a different color, the monthly means denoted by the
566 solid, black line, and +/- 1 standard deviation denoted by the horizontal, black,
567 dashed lines. September of each year is represented by the vertical black, dashed
568 lines.

569
570

571

Atmos. Meas. Tech. Discuss., doi:10.5194/amt-2016-414, 2017
Manuscript under review for journal Atmos. Meas. Tech.
Discussion started: 14 February 2017

Atmospheric Measurement Techniques Discussions

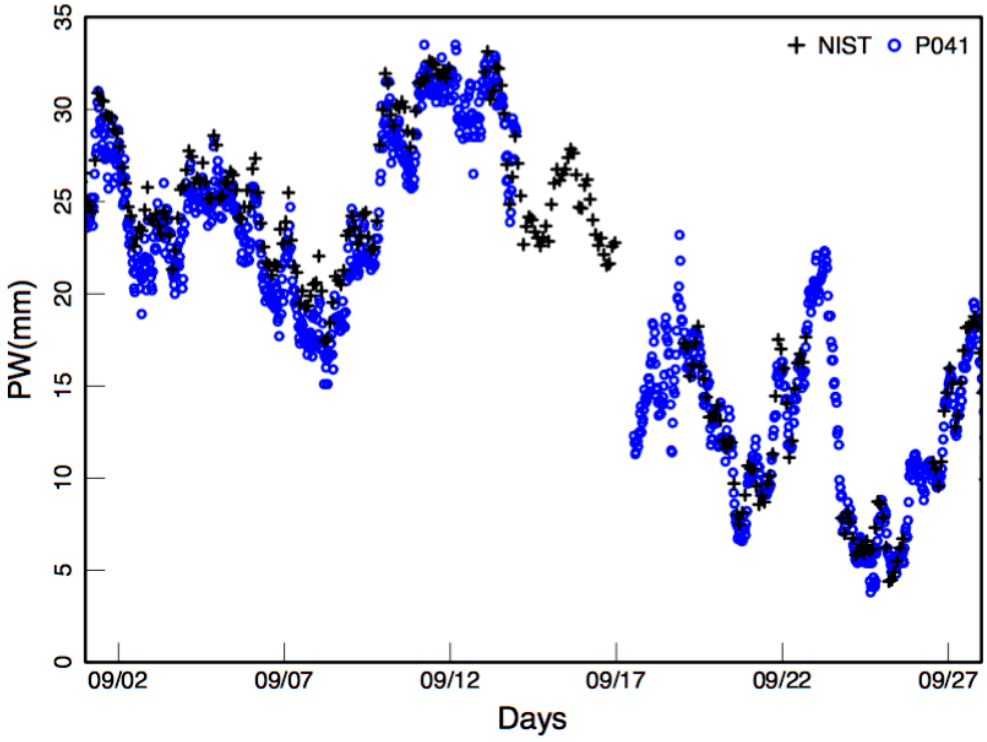

572

573 **Figure 3.** A time series of 30-minute GPS PW (station P041) from 1 – 28 September

574 2013. All times are in UTC.

Atmos. Meas. Tech. Discuss., doi:10.5194/amt-2016-414, 2017
Manuscript under review for journal Atmos. Meas. Tech.
Discussion started: 14 February 2017

Atmospheric Measurement Techniques Discussions

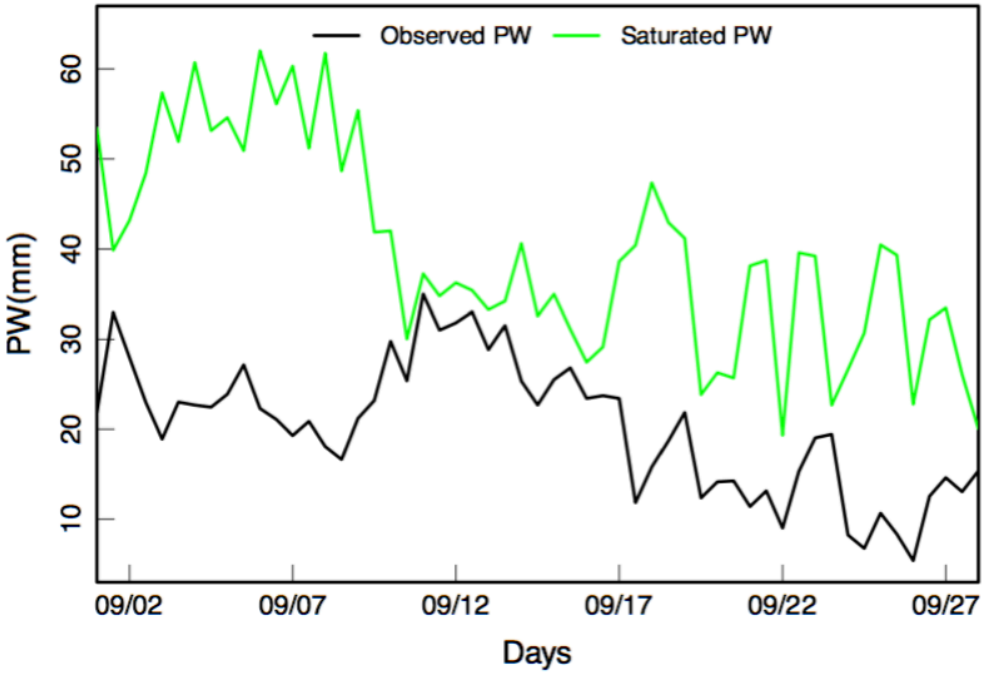

575

576 **Figure 4.** A time series comparison of observed radiosonde PW (black line) and saturated
577 PW (green line) for 1-28 September 2013 over Denver, Colorado. All
578 times are in UTC.

579

580

581

Atmos. Meas. Tech. Discuss., doi:10.5194/amt-2016-414, 2017
Manuscript under review for journal Atmos. Meas. Tech.
Discussion started: 14 February 2017

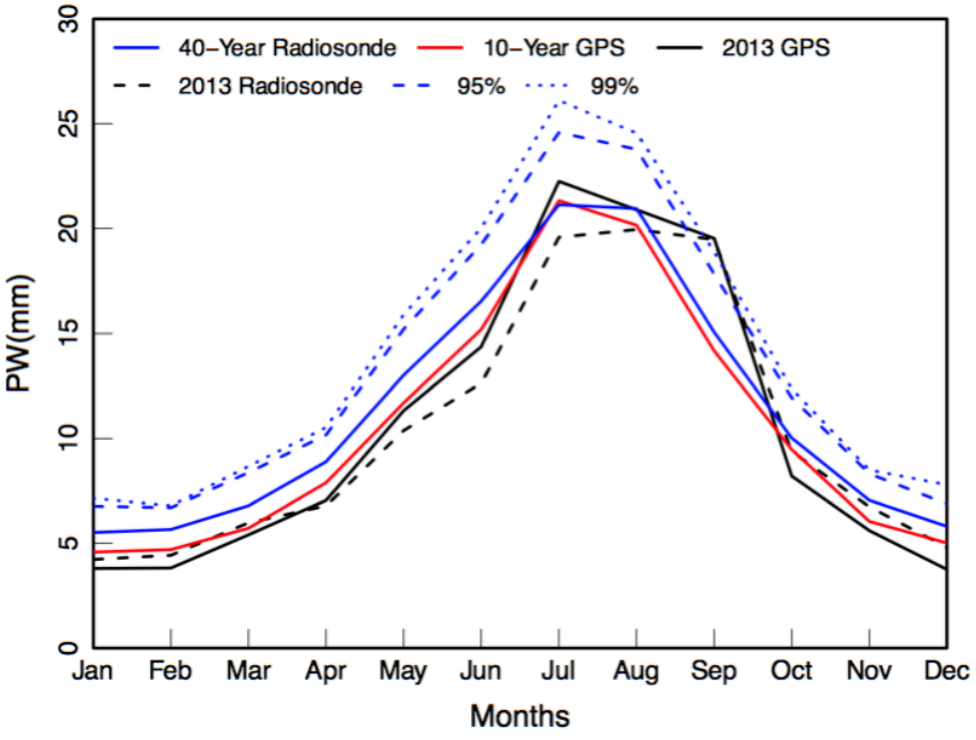

582

583 **Figure 5.** Monthly-averaged GPS PW (solid black line) and Radiosonde data (dashed
584 black line) for 2013 with the 10-year merged GPS PW dataset (solid red line) and the 40-
585 year averaged Radiosonde PW dataset (solid blue line). Additionally, there are the 95th
586 (dashed red line) and 99th (dotted red line) percentiles for 10 years of GPS data and the
587 95th (dashed blue line) and 99th (dotted blue line) percentiles for 40 years of Radiosonde
588 data.

Atmos. Meas. Tech. Discuss., doi:10.5194/amt-2016-414, 2017
Manuscript under review for journal Atmos. Meas. Tech.
Discussion started: 14 February 2017

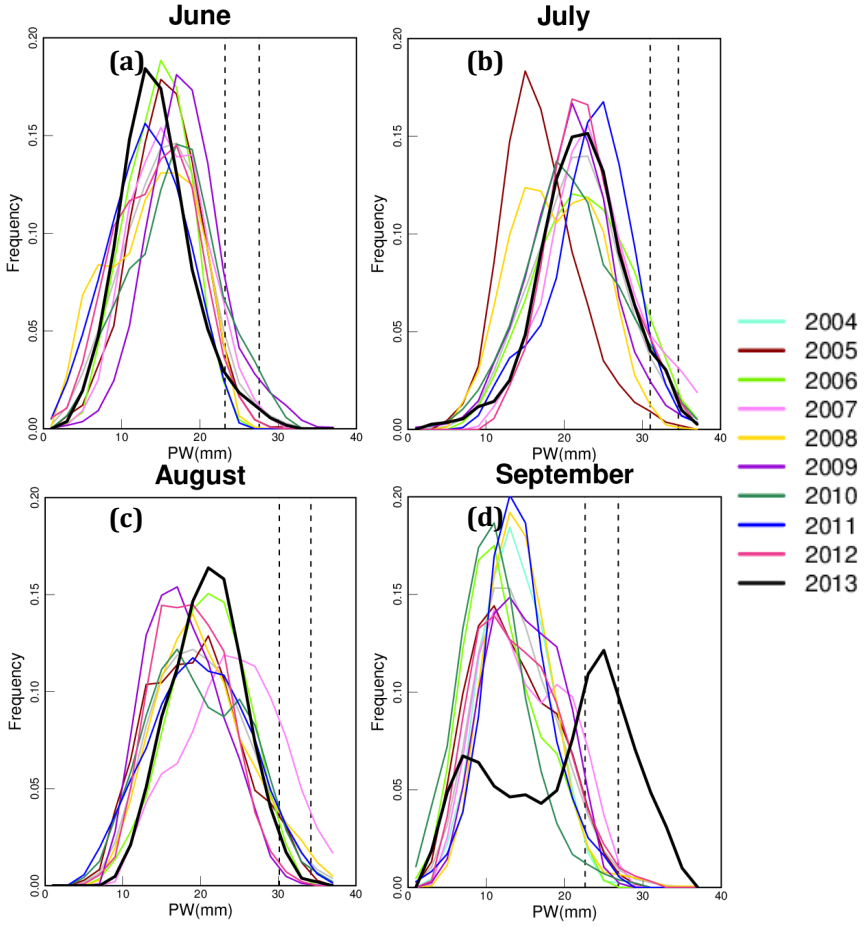

589

590 **Figure 6.** Statistical frequency distributions of GPS PW for June- September of 2004-

591 2013 with the 95th percentile for 10 years of each month of data denoted by the left-most

592 dashed line and the 99th percentile for 10 years of each month of data denoted by the

593 right-most dashed line.

Atmos. Meas. Tech. Discuss., doi:10.5194/amt-2016-414, 2017
Manuscript under review for journal Atmos. Meas. Tech.
Discussion started: 14 February 2017

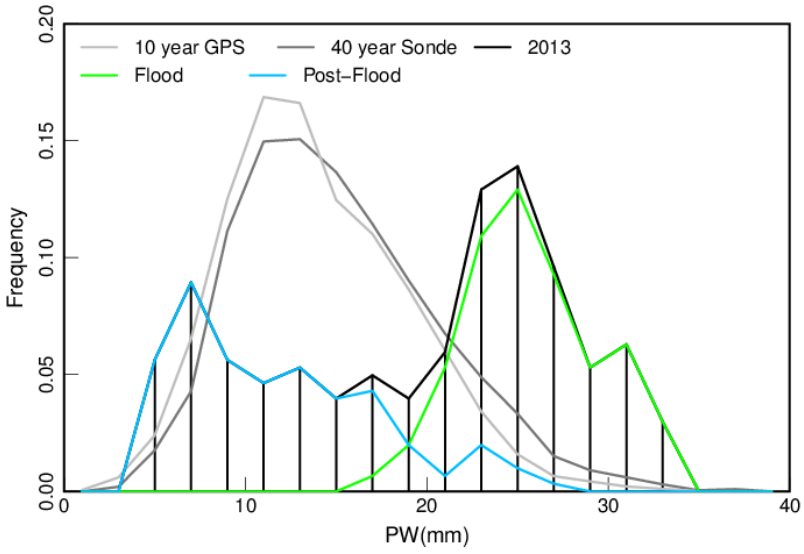

Figure 7. Statistical frequency distributions for the month of September with 2013 GPS PW data over Boulder (black line), 40 years of climatologically-averaged radiosonde PW data over Denver (dark grey line), and 10 years of climatologically-averaged GPS PW data over Boulder (light grey line). September of 2013 GPS PW data was split into two halves: 1-15 September 2013 (Flood; green line), and 16-30 September 2013 (Post-Flood; blue line).

Atmos. Meas. Tech. Discuss., doi:10.5194/amt-2016-414, 2017
Manuscript under review for journal Atmos. Meas. Tech.
Discussion started: 14 February 2017

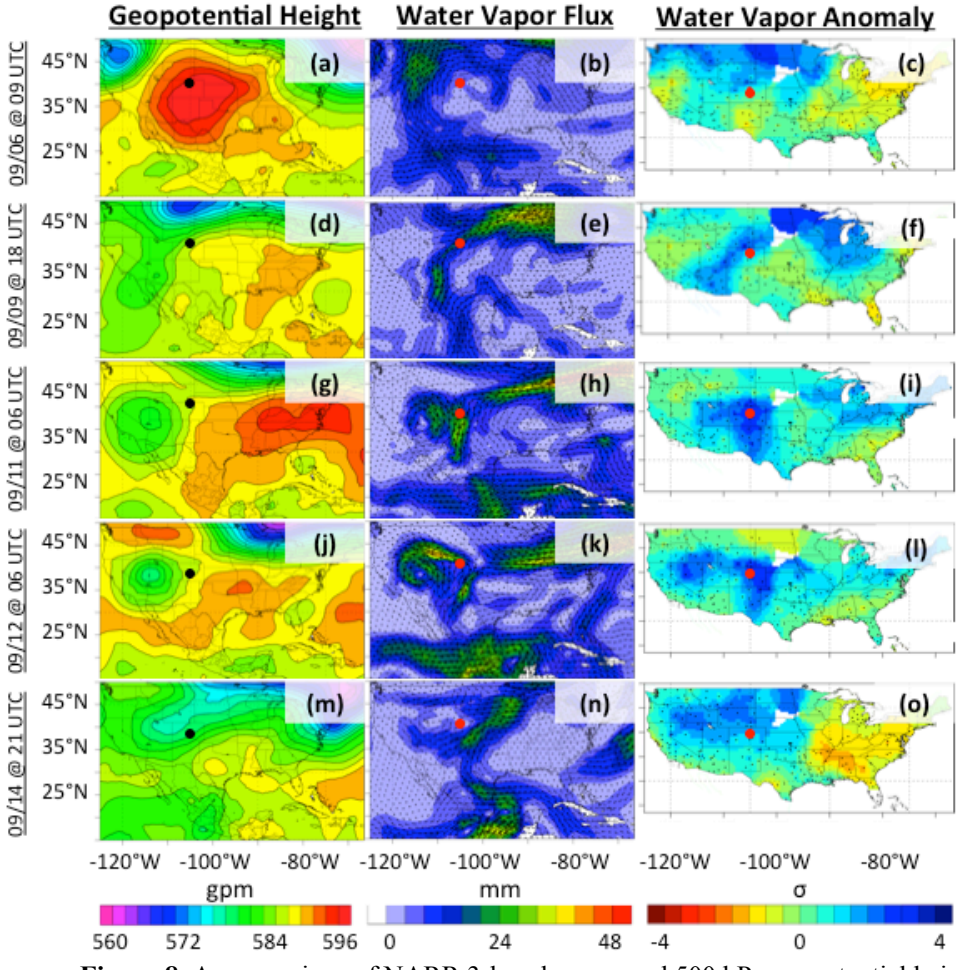

Figure 8. A comparison of NARR 3-hourly averaged 500 hPa geopotential height (left column), NARR 3-hourly averaged integrated water vapor flux (center column), and SuomiNet gridded standardized PW anomalies. Each row represents a different time surrounding the 2013 Event.

Atmos. Meas. Tech. Discuss., doi:10.5194/amt-2016-414, 2017
Manuscript under review for journal Atmos. Meas. Tech.
Discussion started: 14 February 2017

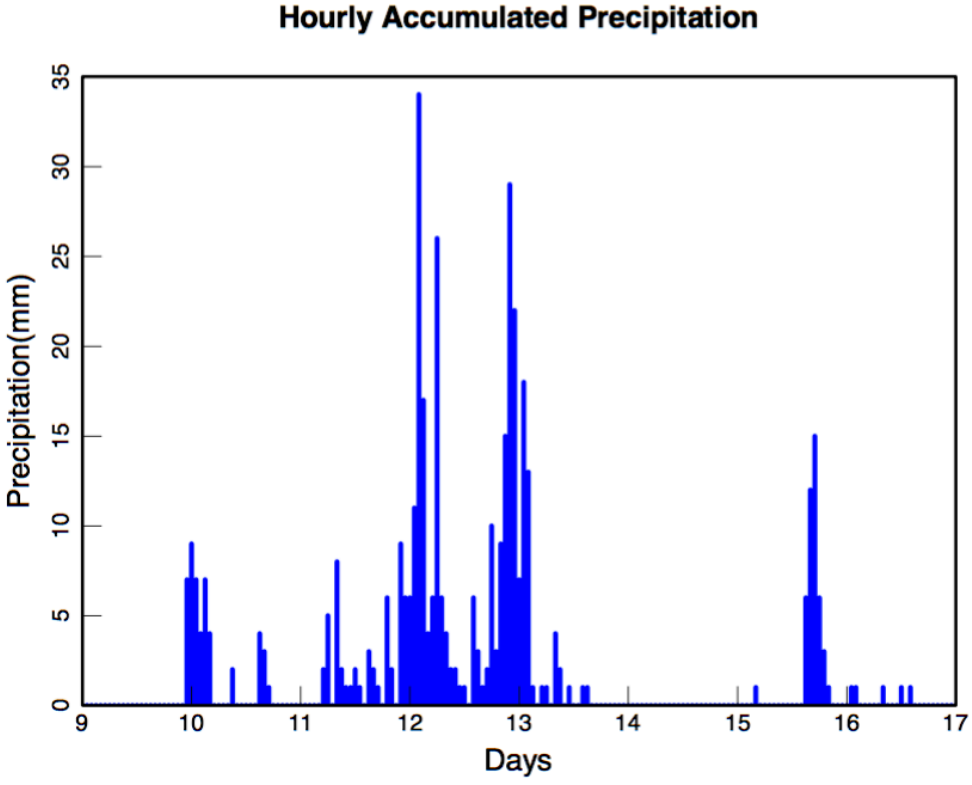

Figure 9. A time series of observed precipitation data from the rain gauge UDFCD_4840 for 9-17 September 2013. All times are in UTC.